Computational Mechanics 19 (1997) 308–316 © Springer-Verlag 1997

A 3-D boundary element formulation of viscoelastic media with gravity

E. Pan, C. Sassolas, B. Amadei, W. T. Pfeffer

Abstract This paper presents a boundary element formulation for 3-D linear and viscoelastic bodies subjected to the body force of gravity. The Laplace transformation is first used to suppress the time variable, and solutions of displacements and stresses are found in the transformed domain. The time domain solutions are then found by an accurate and efficient numerical inversion method which requires only real calculations for all quantities. Input and output data, and solutions in the transformed and time domains are connected through an Interactive Data Language code written by the authors. While particular solutions of stresses and displacements related to the body force of gravity (which is applied at time $t = 0$ and is kept constant) are derived, the Green's functions in the Laplace domain are obtained through the correspondence principle. The new formulation has been implemented into an existing 3-D BEM program, and several numerical examples involving 3-D viscoelastic bodies are presented. Although the discussion in this paper focuses on Maxwell viscoelastic and isotropic media, other linear isotropic and even anisotropic viscoelastic models can also be incorporated, without difficulty, into the 3-D viscoelastic BEM program.

1 Introduction

The solution of problems dealing with the creep and relaxation behavior of polymeric and Earth materials requires that suitable viscoelastic models be available. In order to develop a viscoelastic model, experiments must be conducted as was previously done for rocks (Cristescu, 1993), ice (Schulson et al. 1989), and polymeric materials (Frassine and Pavan, 1990; Huang et al. 1991). Once a viscoelastic model is established, numerical simulations can be run to study the effect of complex geometry and load conditions, as well as material properties, on the response of structures. Since the time variable is involved, the direct analysis in the time domain is usually complicated if a space domain discretization, such as the finite element method, is adopted (Warby et al. 1992). For linear viscoelastic media, however, the boundary element method (BEM) is much more powerful than the domain-discretization method.

Within the BEM context, a viscoelastic problem can be solved either in the time domain directly or in the Laplace-transformed domain with the inversion being carried out later for a given time. For the time domain method, Lee and co-workers (Lee and Westmann, 1995; Lee and Kim, 1995; Lee, 1995) proposed a direct BEM for the analysis of linear viscoelastic media in which the temporal and spatial variables are discretized, and solutions are given in the time domain and space domain simultaneously. For a three-parameter viscoelastic model, Gaul and Schanz (1994) presented a BEM for the calculation of the dynamic response with the time integration being found analytically. Viscoelastic analysis can be also conducted by forming the symmetric boundary integral equations (Carini et al. 1991), which in some cases are computationally more advantageous over the traditional BEM. In all the time-domain approaches, the Green's functions need to be provided in the time domain, for which exact-closed form expressions may not always be possible (Carini and Donato, 1992; Lee et al. 1994). Also, since temporal and spatial discretizations are usually required simultaneously in the time-domain approach, data files are one dimension larger than those for the corresponding static 3-D problem. Another concern involved with the time-domain method is the effect of previous time-step integral on the subsequent steps.

An alternative technique, called the Laplace transformed BEM method, uses the correspondence principle (Lee, 1955; Schapery, 1965). The problem is solved in the Laplace domain first, and then inverted to the time domain for the given time point. This approach was used by Kusama and Mitsui (1982), Wang and Clouch (1982), and Carini and Gioda (1986) for 2-D viscoelastic problems. Since in this approach, the Green's functions are provided in exact closed-form, more accurate results can be obtained than with the time-domain method. This approach has been applied to different types of time-dependent linear problems (Narayanan and Beskos, 1982). To the authors knowledge, however, this method has been applied mostly to 2-D viscoelastic media. No application of this method to 3-D viscoelastic problems has appeared in the

Communicated by S. N. Atluri, 26 August 1996

E. Pan, B. Amadei
University of Colorado, Dept. of Civil Engineering,
Boulder, CO 80309-0428, USA

C. Sassolas, W.T. Pfeffer
Institute of Arctic and Alpine Research, Boulder,
CO 80309-0450, USA

Correspondence to: E. Pan

The authors are grateful for the supports of the Department of Energy under grant DE-FG 03-93-ER61689 and of the National Science Foundation under grant CMS-9622645.

literature, nor have applications appeared which involve the body force of gravity.

This paper, following the Laplace transformed method, presents a BEM formulation for 3-D linear viscoelastic bodies subject to gravity. The body force of gravity is assumed to be applied at time $t = 0$ and to remain constant afterwards. Particular solutions of displacements and stresses related to this body force in the Laplace transformed domain are derived in exact closed-form for generally anisotropic viscoelastic media. The Green's functions in the transformed domain are obtained from the pure static elastic ones (Pan and Amadei, 1996) by replacing the elastic constants with the corresponding Laplace variable dependent coefficients following the correspondence principle (Lee, 1955). Discretization of the BEM formulation in the Laplace transformed domain follows exactly that for the pure static elastic case (Pan and Amadei, 1996), and inversion to the time-domain is achieved by an accurate and efficient numerical inversion method (Piessens, 1972; Hanggi et al, 1980; Chave, 1983). Input and output data, and solutions in the transformed and time domains are connected through an Interactive Data Language (IDL) code written by the authors. Furthermore, a data compressing algorithm is also implemented which allows large memory savings for files which are not currently in use. Numerical examples are presented to show the accuracy and efficiency of the method.

2
Formulation in Laplace domain

Consider a viscoelastic body as shown in Figure 1 and let x, y, z (or x_1, x_2, x_3) be a global coordinate system. This body is subjected to time-dependent body forces $B_i(x_j; t)(i = 1, 2, 3)$, boundary tractions on Γ_t and boundary displacements on Γ_u (Fig. 1). Within the body, the displacement and stress fields must satisfy the governing equations in the time domain.

Assuming a zero initial condition for the problem under consideration, we therefore can employ the Laplace transform to suppress the time variable. That is, we can apply the following transform

$$F(s) = \int_0^\infty f(t)e^{-st}\mathrm{d}t \tag{1}$$

to the time-dependent governing equations as well as the boundary conditions.

With the transformation (1), one can find that in the Laplace transformed domain, the following equations as well as the boundary conditions must be satisfied.

Equations of equilibrium

$$\sigma_{ij,j}(x_k; s) + B_i(x_k; s) = 0 \tag{2}$$

Constitutive relations

$$[\sigma(x_k; s)] = [c(s)][e(x_k; s)] \tag{3}$$

with

$$\begin{aligned}[\sigma(x_k; s)] &= [\sigma_{11}, \sigma_{22}, \sigma_{33}, \sigma_{32}, \sigma_{31}, \sigma_{12}]^t \\ [e(x_k; s)] &= [e_{11}, e_{22}, e_{33}, 2e_{32}, 2e_{31}, 2e_{12}]^t\end{aligned} \tag{4}$$

and $[c(s)]$ being the elastic stiffness matrix of the body in the Laplace transformed domain. These Laplace transformed elastic constants are derived in Appendix A for the generalized Kelvin model, and for the Maxwell model as a special case.

Displacement and strain relations

$$e_{ij}(x_k; s) = 0.5[u_{i,j}(x_k; s) + u_{j,i}(x_k; s)] \tag{5}$$

The displacements and stresses must also satisfy the following boundary conditions

$$\begin{aligned}u_i(x_k; s) &= \overline{u_i(x_k; s)}; \qquad x_k \in \Gamma_u \\ \sigma_{ij}n_j(x_k; s) &= \overline{T_i(x_k; s)}; \qquad x_k \in \Gamma_t\end{aligned} \tag{6}$$

Because the problem is linear, the total displacements and stresses in the Laplace transformed domain can be expressed as follows

$$\begin{aligned}u_i^t &= u_i^h + u_i^p \\ \sigma_{ij}^t &= \sigma_{ij}^h + \sigma_{ij}^p \\ T_i^t &= T_i^h + T_i^p\end{aligned} \tag{7}$$

where the superscript t denotes the total solution, h the homogeneous solution, and p a particular solution corresponding to the body forces B_i.

Following the procedure by Pan and Amadei (1996), one can show that the internal total displacement solution can be expressed by the following integral:

$$\begin{aligned}u_i^t(\boldsymbol{x}_p; s) + \int_\Gamma T_{ij}^*(\boldsymbol{x}_p, \boldsymbol{x}; s)u_j^t(\boldsymbol{x}; s)\mathrm{d}\Gamma(\boldsymbol{x}) &= \int_\Gamma U_{ij}^*(\boldsymbol{x}_p, \boldsymbol{x}; s)T_j^t(\boldsymbol{x}; s)\mathrm{d}\Gamma(\boldsymbol{x}) \\ &+ u_i^p(\boldsymbol{x}_p; s) + \int_\Gamma T_{ij}^*(\boldsymbol{x}_p, \boldsymbol{x}; s)u_j^p(\boldsymbol{x}; s)\mathrm{d}\Gamma(\boldsymbol{x}) \\ &- \int_\Gamma U_{ij}^*(\boldsymbol{x}_p, \boldsymbol{x}; s)T_j^p(\boldsymbol{x}; s)\mathrm{d}\Gamma(\boldsymbol{x})\end{aligned} \tag{8}$$

with U_{ij}^* and T_{ij}^* being the Green's displacements and tractions in the Laplace transformed domain. These Green's solutions can be obtained from the pure static elastic solutions (Pan and Amadei, 1996) by simply replacing the elastic constants with the Laplace variable dependent coefficients following the correspondence principle.

Let $\boldsymbol{x}_p$ approach a point $\boldsymbol{y}$ on the boundary, we finally obtain the following boundary integral equation

$$\begin{aligned}b_{ij}u_i^t(\boldsymbol{y}; s) + \int_\Gamma T_{ij}^*(\boldsymbol{y}, \boldsymbol{x}; s)u_j^t(\boldsymbol{x}; s)\mathrm{d}\Gamma(\boldsymbol{x}) &= \int_\Gamma U_{ij}^*(\boldsymbol{y}, \boldsymbol{x}; s)T_j^t(\boldsymbol{x}; s)\mathrm{d}\Gamma(\boldsymbol{x}) \\ &+ \int_\Gamma T_{ij}^*(\boldsymbol{y}, \boldsymbol{x}; s)[u_j^p(\boldsymbol{x}; s) - u_i^p(\boldsymbol{y}; s)]\mathrm{d}\Gamma(\boldsymbol{x}) \\ &- \int_\Gamma U_{ij}^*(\boldsymbol{y}, \boldsymbol{x}; s)T_j^p(\boldsymbol{x}; s)\mathrm{d}\Gamma(\boldsymbol{x})\end{aligned} \tag{9}$$

where b_{ij} are coefficients that depend only upon the local geometry of the boundary at y.

It is noted that all the terms on the right hand side of Equ. (9) have only weak singularities. Thus, this equation is integrable. Although the second term on the left hand side of Equ. (9) has a strong singularity, it can be treated by the rigid-body motion method. At the same time, the calculation of b_{ij}, which is geometry dependent, can also be avoided.

Using the boundary conditions (6), Equ. (9) in the Laplace transformed domain can be discretized and solved numerically for the unknown boundary displacements and tractions. Then Equ. (8) can be used to calculate the internal displacements. In order to calculate the internal stresses, we need to first take the derivative of Equ. (8) with respect to the internal coordinates x_p. This procedure results in the following equation:

$$\begin{aligned} u^t_{i,k}(x_p;s) &+ \int_\Gamma T^*_{ij,k}(x_p,x;s)u^t_j(x;s)\mathrm{d}\Gamma(x) \\ &= \int_\Gamma U^*_{ij,k}(x_p,x;s)T^t_j(x;s)\mathrm{d}\Gamma(x) \\ &+ \int_\Gamma T^*_{ij,k}(x_p,x;s)[u^p_j(x;s) - u^p_i(x_p;s)]\mathrm{d}\Gamma(x) \\ &- \int_\Gamma T^*_{ij}(x_p,x;s)u^p_{j,k}(x_p;s)\mathrm{d}\Gamma(x) \\ &- \int_\Gamma U^*_{ij,k}(x_p,x;s)T^p_j(x;s)\mathrm{d}\Gamma(x) \qquad (10) \end{aligned}$$

Once the $u^t_{i,k}$ are obtained, Eqs. (3)–(5) can be used to calculate the internal stresses. It is noted that in Eqs. (8) and (10), the particular solutions of displacements and stresses (tractions), as well as the Green's displacements and stresses need to be provided. While the Green's solutions can be obtained directly from the corresponding elastic solutions through the correspondence principle, we will, in the following section, present the particular solution associated with the body force of gravity acting in a general orientation with respect to the x, y, z coordinate system of Figure 1.

3
Particular solutions in the Laplace domain

The body force of gravity is applied at time $t = 0$ to the viscoelastic body of Fig. 1 and is assumed to remain constant afterwards. Following the same procedure as in Amadei and Pan (1992) and Pan and Amadei (1996), a very simple and exact closed-form particular solution related to the body force of gravity can be derived. In the Laplace transformed domain, the particular displacements are:

$$\begin{aligned} u^p_1(x_k;s) &= a_1B_1(s)x_1^2 + b_1B_2(s)x_2^2 + c_1B_3(s)x_3^2 \\ u^p_2(x_k;s) &= a_2B_1(s)x_1^2 + b_2B_2(s)x_2^2 + c_2B_3(s)x_3^2 \qquad (11) \\ u^p_3(x_k;s) &= a_3B_1(s)x_1^2 + b_3B_2(s)x_2^2 + c_3B_3(s)x_3^2 \end{aligned}$$

where for brevity, the dependence of a_i, b_i, and c_i on the Laplace variable s has been omitted. Their relations to the Laplace transformed elastic coefficients are given in Appendix B. The Laplace transformed body force $B_i(s)$ is given by

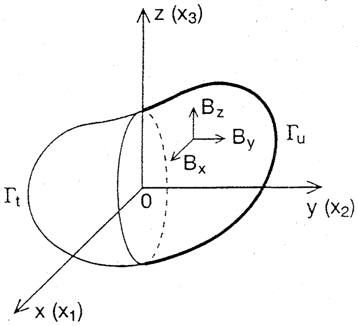

Fig. 1. Geometry of the problem. A 3-D viscoelastic region with body forces $B_i(x_k, t)$. On boundaries Γ_u and $\Gamma_t (\Gamma = \Gamma_u + \Gamma_t)$, time-dependent displacements and tractions are described respectively

$$B_i(s) = \rho g_i / s; \qquad i = 1,2,3 \qquad (12)$$

Similarly, the particular stresses can be expressed as

$$\begin{bmatrix} \sigma^p_{11} \\ \sigma^p_{22} \\ \sigma^p_{33} \\ \sigma^p_{23} \\ \sigma^p_{13} \\ \sigma^p_{12} \end{bmatrix} = \begin{bmatrix} d_{11} & d_{12} & d_{13} \\ d_{21} & d_{22} & d_{23} \\ d_{31} & d_{32} & d_{33} \\ d_{41} & d_{42} & d_{43} \\ d_{51} & d_{52} & d_{53} \\ d_{61} & d_{62} & d_{63} \end{bmatrix} \begin{bmatrix} B_1(s)x_1 \\ B_2(s)x_2 \\ B_3(s)x_3 \end{bmatrix} \qquad (13)$$

Again, the d_{ij} depend on the Laplace transformed elastic coefficients which are given in Appendix B.

4
Numerical methods for Laplace inversion transform

Various methods have been proposed in the literature for the numerical inversion of the Laplace transform. A review of these methods can be found in Davies and Martin (1979) and Narayanan and Beskos (1982). While Talbot's method (1979) is very accurate and efficient, it requires that the Laplace transformed function $F(s)$ be in the complex plane. For the 3-D viscoelastic problems presented above, this means a lot of computational time since one needs to solve the BEM formulation in the complex plane and almost all the quantities involved need to be complex. By restricting the Laplace transformed functions $F(s)$ to the real axis, the most efficient method is the one presented by Piessens (1972), which has been verified by Davies and Martin (1979). In this method, the Laplace transformed function $F(s)$ is approximated by the Chebyshev polynomials T_n as

$$F(s) = s^{-\alpha-1}\sum_{n=0}^{N} a_n T_n(1 - b/s) \qquad (14)$$

Inverting the series term by term, the corresponding time-domain function is

$$f(t) = t^\alpha(\alpha!)^{-1}\sum_{n=0}^{N} a_n \phi_n(bt/2) \qquad (15)$$

In the above two equations, α and b are parameters. While α is related to the asymptotic behavior of $F(s)$ for large s, b is related to the accuracy chosen (Piessens, 1972; Davies and Martin, 1979). Our test of the Laplace inversion program revealed that $\alpha = 0$ and $b = 0.075$ gave good results. Also in these two equations, a_n are coefficients and $\phi_n(x)$ is a polynomial of degree n. The coefficients a_n are given by

$$a_0 = \frac{1}{N+1}\sum_{n=0}^{N} \Phi\left[\cos\left(\frac{(2n+1)\pi}{2(N+1)}\right)\right] \tag{16a}$$

$$a_k = \frac{2}{N+1}\sum_{n=0}^{N} \Phi\left[\cos\left(\frac{(2n+1)\pi}{2(N+1)}\right)\right]\cos\left(\frac{(2n+1)k\pi}{2(N+1)}\right) \tag{16b}$$

$$\Phi(r) = \left(\frac{b}{1-r}\right)^{\alpha+1} F\left(\frac{b}{1-r}\right) \tag{16c}$$

The first three polynomials $\phi_n(x)(n = 0, 1, 2)$ are equal to

$$\begin{aligned} \phi_0(x) &= 1 \\ \phi_1(x) &= 1 - \frac{2x}{\alpha+1} \\ \phi_2(x) &= 1 - \frac{8x}{\alpha+1} + \frac{8x^2}{(\alpha+1)(\alpha+2)} \end{aligned} \tag{17}$$

For $n > 2$, the recurrence relations for $\phi_n(x)$ are

$$\begin{aligned} -\phi_n(x) = (A + Bx)\phi_{n-1}(x) + (C + Dx)\phi_{n-2}(x) \\ + E\phi_{n-3}(x) \end{aligned} \tag{18}$$

with

$$\begin{aligned} A &= 2n + \frac{(n-1)(2n-3)(\alpha+n-1)}{(n-2)(\alpha+n)} \\ B &= 4/(\alpha+n) \\ D &= \frac{4(n-1)}{(n-2)(\alpha+n)} \\ E &= \frac{(n-1)(\alpha-n+3)}{(n-2)(\alpha+n)} \\ C &= -1 - A - E \end{aligned} \tag{19}$$

When summing up the $f(t)$, the continued fraction expansion method (Hanggi et al, 1980; Chave, 1983) is introduced so that the original series is transformed into one that converges very rapidly. Therefore, the Laplace inversion transform can be evaluated with considerable accuracy using relatively few determinations of the Laplace transform itself.

5
Code implementation

As mentioned above we have developed an efficient way to conduct 3-D viscoelastic analysis in the Laplace domain, and to give the results for several values of the Laplace variable s. In so doing, the time-step integral problem has been avoided and the data file structure is the same as for the corresponding pure static elastic 3-D case. However, we must have different files for different values of the Laplace variable, which means that the 3-D BEM program itself still involves large data files. To take full advantage of the main characteristic of the BEM (i.e. spatial discretization on the problem boundary only) and of the Piessens and continued fraction expansion methods as explained above (i.e. accurate result with a few determinations of the Laplace transform), an IDL code was written and used by the authors as an interface between the main computational units.

For a given 3-D viscoelastic problem, we first transform the problem into the Laplace domain. We discretize the spatial domain with l nodes $(x_i, y_i, z_i; i = 1 \rightarrow l)$. We then run the Laplace transformed 3-D BEM program *visco3d.for* for m Laplace variables $(s_j; j = 1 \rightarrow m)$. These analyses result in m files (one for each Laplace variable s) containing l lines (one for each space point) of displacements and stresses (Fig. 2a). To apply the numerical Laplace inversion transform, we rearrange the data in such a way that each spatial point $(i = 1 \rightarrow l)$ is linked to m values of a component of the displacement or stress (each corresponding to a given Laplace variable s). The numerical inversion Laplace transform program, which is based on the Piessens and continued fraction expansion methods, *invlap.for* is then run for n specific time points (Fig. 2b). At this point, the original files containing the results in the Laplace domain are no longer necessary and can be erased.

The final result consists of displacement and stress values for l spatial points at each time. The overall algorithm is very efficient in saving both computational time and memory, allowing a better accuracy and application on increased sized geometry.

6
Numerical examples

The boundary integral equation in the Laplace transformed domain (11) was solved numerically using a 3-D BEM program written and modified by the authors (Pan and Amadei, 1996). In this program, the boundary of the continuum is discretized into nine-node quadrilateral curved elements. The displacements and tractions on the boundary of each element are expressed in terms of their corresponding node values by nine-node quadrilateral shape functions. Assuming isoparametric elements, the coordinates at any point in an element are related to the element nodal coordinates in the same way as for displacements or tractions.

The Maxwell viscoelastic model was used in all the examples with the material properties being $\rho g = 27 \times 10^3$ Pa/m, $\lambda = \mu = 1.6 \times 10^7$ Pa, and $\nu = 10^8$ Pa-day (Cristescu, 1993). For each example, only six elements with a total of 26 nodes were used to discretize the entire problem boundary. Also, only six Laplace variable points $(m = 6)$ were used to invert the transformation.

The first example is a cubical block, 1 m in size, subjected to uniaxial and uniform compression $T \cdot H(t)$ in the z-direction (Fig. 3a) where $H(t)$ is the Heaviside function and $T = 1$ kPa. For this case, exact closed-form solutions of displacements and stresses can be found and are given

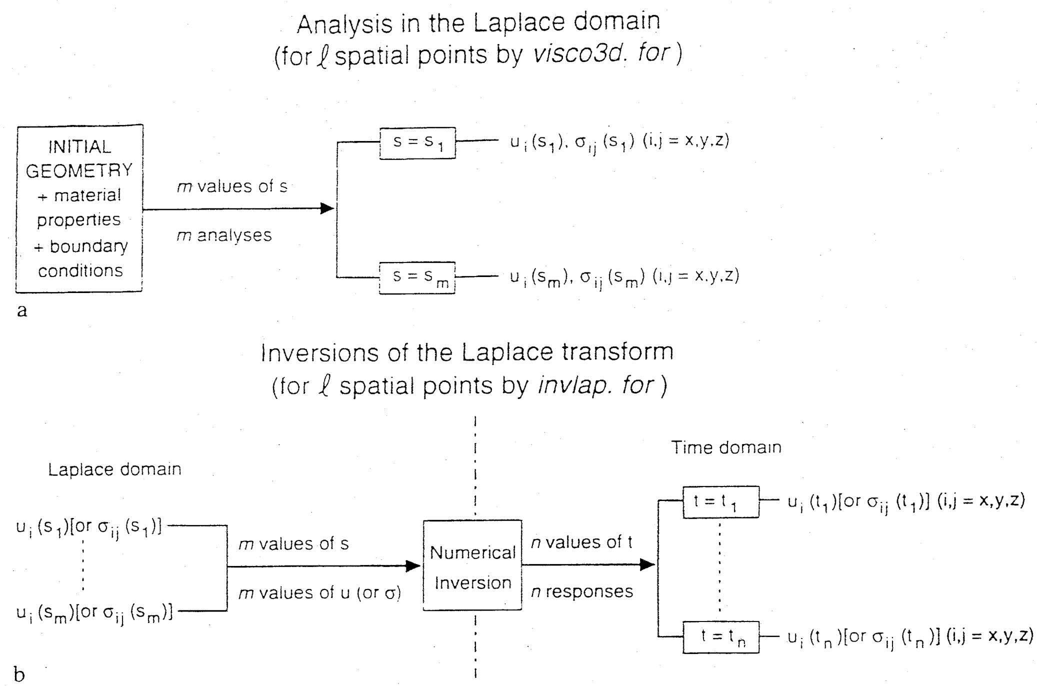

Fig. 2a,b. Scheme of analysis in the Laplace and time domains

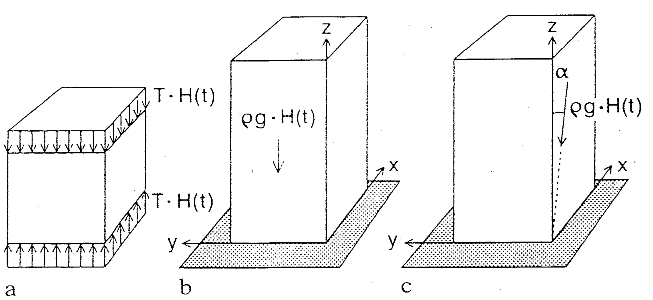

Fig. 3a–c. Block under uniform vertical compression $T \cdot H(t)$ in (a); Block on a rigid base under gravity $\rho g \cdot H(t)$ in (b) and in xz plane inclined 5 degrees to the z-direction (c)

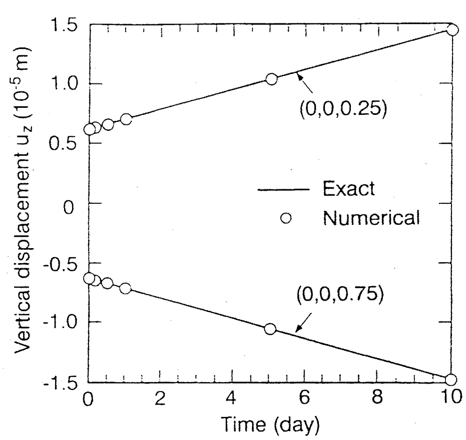

Fig. 4. Variation of internal vertical displacement u_z at (0, 0, 0.25) and (0, 0, 0.75) with time t, caused by the uniform compression $T \cdot H(t)$

in Appendix C. The displacement in the z-direction for different times t at the top surface of the block in Fig. 3a is given in Table 1. It can be seen that the numerical displacements are identical, to five significant digits, to those of the exact closed-form solutions. Figure 4 shows the internal displacement in the vertical direction u_z at points (0, 0, 0.25 m) and (0, 0, 0.75 m) on the central line of the block. This figure indicate that the numerical results and the exact solutions are in excellent agreement. We have also checked the internal stress component σ_{zz} along the central line of the block. The exact solution for this stress component is $H(t)$ (kPa) for $T = 1$. It was found that our numerical results agreed with this value for $t = 0$, $0.1, 0.5, 1, 5, 10$ (day) up to five significant digits.

The second example corresponds to a prismatic block ($1 \times 1 \times 2$ m) resting on a rigid base and subject to the body force of gravity $\rho g \cdot H(t)$ in the vertical direction (Fig. 3b). For this case, no exact closed-form solution is available. However, an analytical solution exists on the basis of St. Venant's principle, and the solution is derived in Appendix C. The vertical displacement u_z at the top center of the block (Fig. 3b) for different times is given in Table 2. This table indicate that both the numerical and St. Venant's solutions are in good agreement. It is noteworthy that for $t = 0$ (corresponding to the pure elastic solution), the vertical displacement calculated by our pure elastic 3-D BEM program (Pan and Amadei, 1996) is $-1.33(\times 10^{-3}$ m) which is very close to the result obtained using our current viscoelastic program. Fig. 5 shows the displacement in the vertical direction $u_z(m)$ at different

Table 1. Surface displacement u_z ($\times 10^{-5}$ m) for a block under uniform compression

t (day)	0.0	0.1	0.5	1.0	5.0	10.0
Number.	−1.2500	−1.2667	−1.3333	−1.4167	−2.0833	−2.9167
Exact	−1.2500	−1.2667	−1.3333	−1.4167	−2.0833	−2.9167

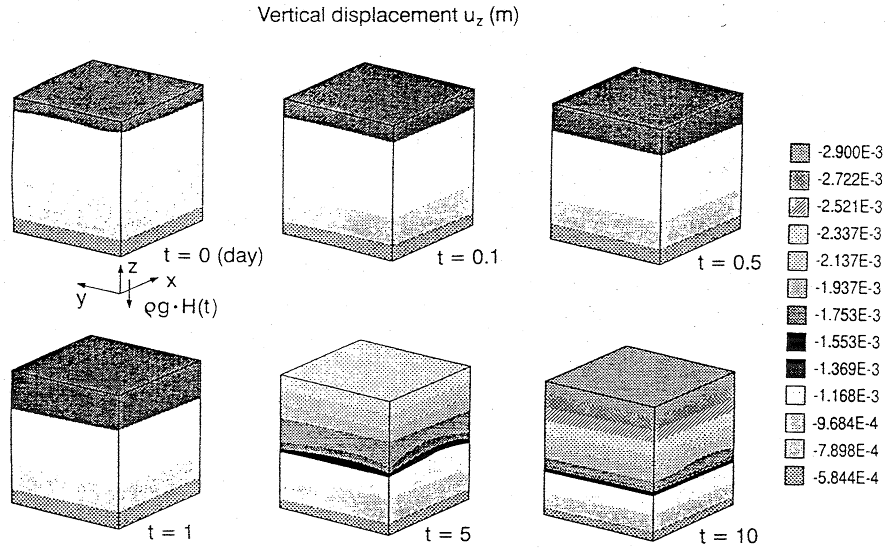

Fig. 5. Variation of vertical displacement u_z (in m) with time t (in days) for a block under gravity $\rho g \cdot H(t)$ in vertical direction (Fig. 3b)

Table 2. Vertical displacement u_z ($\times 10^{-3}$ m) for a viscoelastic block on a rigid base under gravity in the vertical direction

t (day)	0.0	0.1	0.5	1.0	5.0	10.0
Numer.	−1.3284	−1.3447	−1.4097	−1.4907	−2.1288	−2.9057
St. Venant's	−1.3500	−1.3680	−1.4400	−1.5300	−2.2500	−3.1500

times. As expected, the absolute value of the displacement increases with increasing time, with the largest displacement being at the top surface of the block. For this special case, the stress component σ_{zz} is constant with respect to time. It changes, however, with respect to the space variable. For example, Fig. 7a shows the distribution of the stress component σ_{zz} in the block at $t = 0$. We can see that, this stress component is zero at the top surface and reaches a maximum value at the bottom.

A third and final example corresponds to the case of a block resting on a rigid base subject to the body force of gravity $\rho g \cdot H(t)$ acting in the xz plane and inclined 5 degrees to the z-direction (Fig. 3c). This is equivalent to a block tilted at 5 degrees from the horizontal around the y-axis and subject to the body force of gravity $\rho g \cdot H(t)$ in the vertical direction. The displacement u_z at different time steps and the stress component σ_{zz} at $t = 0$ are shown, respectively, in Figs. 6 and 7b. Compared to the vertical block case (Fig. 5 and 7a), the effect of block inclination on the displacement and stress fields is obvious.

7
Conclusions

In this paper, we present a 3-D BEM formulation for the analysis of linear viscoelastic isotropic media. Particular solutions in the Laplace transformed domain for the body force of gravity applied in a general orientation are derived in an *exact closed-form*, and are incorporated rigorously into the boundary element formulation. The boundary value problem with zero-initial condition is first solved in the Laplace transformed domain, and then inverted back to the time domain by an accurate and efficient numerical Laplace inverse method.

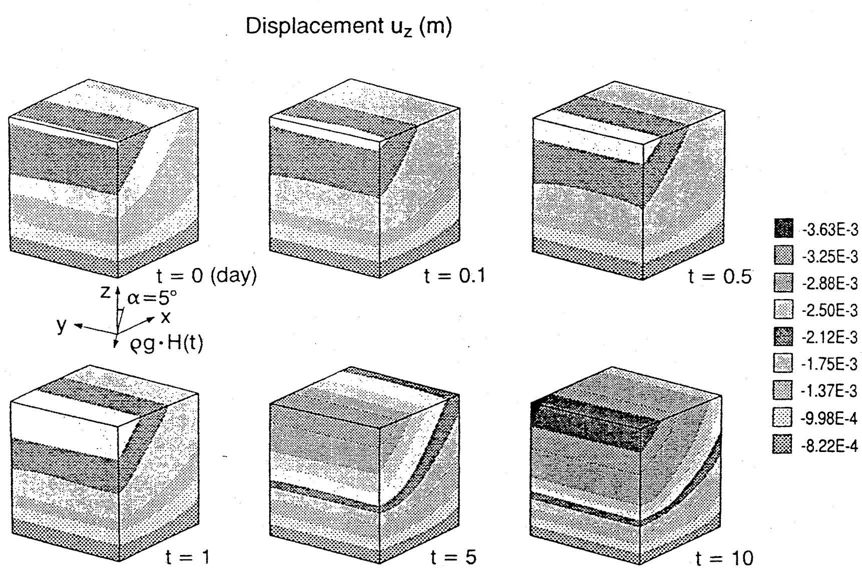

Fig. 6. Variation of displacement u_z (in m) with time t (in days) for a block under gravity $\rho g \cdot H(t)$ inclined 5 degrees with respect to the z-direction (Fig. 3c)

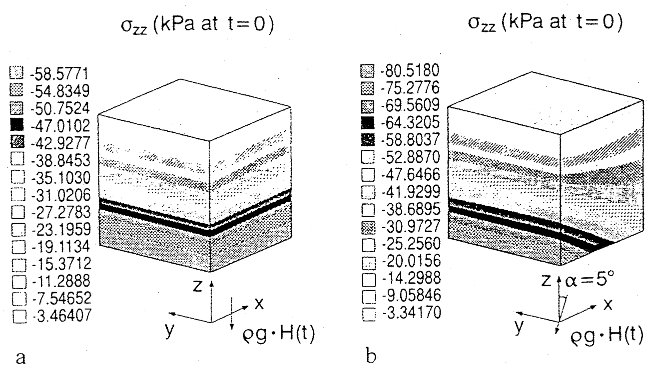

Fig. 7a,b. Distribution of stress σ_{zz} (in kPa) at time $t = 0$ in a block under gravity $\rho g \cdot H(t)$ in vertical direction (a) and inclined 5 degrees to the z-direction (b)

Several numerical examples were studied and carefully checked with existing closed-form solutions. It is found that even with a very coarse discretization and very few Laplace points, excellent results can be obtained.

The present viscoelastic 3-D BEM formulation has applications in geotechnical engineering and in material and Earth sciences. An example of applications includes the determination of displacements and stresses in a viscoelastic and gravity-loaded finite body with complex geometry and boundary conditions. A subject of interest to the authors at the present time is the determination of displacement and stress fields in glacier ice. Another example of applications is the analysis of the time-dependent response of a viscoelastic medium induced by excavation in an infinite domain subjected to triaxial far-field stresses. Finally, our model can be used to predict the creep and relaxation of polymeric materials. Although this paper is focused on the linear, isotropic Maxwell model, other linear, isotropic and even anisotropic viscoelastic models can be easily included in our program. Studies of anisotropic and viscoelastic models were conducted by Christen (1987) and Han (1993), and applied to Earth science related topics such as anisotropic viscosity of Earth's mantle and glacial movement.

Appendix

A

Viscoelastic constitutive relations for a generalized Kelvin model can be expressed as (Carini and Gioda, 1986; Carini and Donato, 1992)

$$\begin{aligned} \sum_{n=0}^{N} a_n \frac{\partial^n \sigma_{kk}}{\partial t^n} &= \sum_{n=0}^{N} b_n \frac{\partial^n e_{kk}}{\partial t^n} \\ \sum_{n=0}^{N} c_n \frac{\partial^n \tau_{kl}}{\partial t^n} &= \sum_{n=0}^{N} d_n \frac{\partial^n \varepsilon_{kl}}{\partial t^n} \end{aligned} \tag{A1}$$

where, σ_{kk} and e_{kk} are hydrostatic parts of the stress and strain tensors, and τ_{kl} and ε_{kl} are the components of the stress and strain deviators. After Laplace transform, we have

$$\begin{aligned} \sigma_{kk}(s) &= 3K(s)e_{kk}(s) \\ \tau_{kl}(s) &= 2\mu(s)\varepsilon_{kl}(s) \end{aligned} \tag{A2}$$

where $K(s)$ and $\mu(s)$ are equivalent bulk and shear moduli, respectively, and are given by

$$\begin{aligned} K(s) &= \frac{1}{3}\sum_{n=0}^{N} b_n s^n \Big/ \sum_{n=0}^{N} a_n s^n \\ \mu(s) &= \frac{1}{2}\sum_{n=0}^{N} d_n s^n \Big/ \sum_{n=0}^{N} c_n s^n \end{aligned} \tag{A3}$$

Equation (A2) can also be written in terms of the equivalent Lame coefficients as

$$\sigma_{ij}(s) = \lambda(s)u_{k,k}\delta_{ij} + \mu(s)(u_{i,j} + u_{j,i}) \tag{A4}$$

where

$$\lambda(s) = K(s) - 2\mu(s)/3 \tag{A5}$$

For a Maxwell model with no dissipation of compression energy, one can find that (Carini and Donato, 1992):

$$\begin{aligned} \lambda(s) &= (\lambda s + \mu K/v)/(s + \mu/v) \\ \mu(s) &= \mu s/(s + \mu/v) \\ K &= \lambda + 2\mu/3 \end{aligned} \tag{A6}$$

where λ and μ are elastic Lame parameters, and v is the absolute (dynamic) viscosity.

B

In the particular solution of the displacement caused by the body force of gravity, i.e. Eqn. (11), the coefficients are

$$\begin{aligned} a_1 &= 0.5(c_{55}c_{66} - c_{56}c_{56})/\Delta_1 \\ a_2 &= 0.5(c_{15}c_{56} - c_{55}c_{16})/\Delta_1 \\ a_3 &= 0.5(c_{16}c_{56} - c_{15}c_{66})/\Delta_1 \end{aligned} \tag{B1}$$

$$\begin{aligned} b_1 &= 0.5(c_{24}c_{46} - c_{26}c_{44})/\Delta_2 \\ b_2 &= 0.5(c_{44}c_{66} - c_{46}c_{46})/\Delta_2 \\ b_3 &= 0.5(c_{26}c_{46} - c_{24}c_{66})/\Delta_2 \end{aligned} \tag{B2}$$

$$\begin{aligned} c_1 &= 0.5(c_{34}c_{45} - c_{35}c_{44})/\Delta_3 \\ c_2 &= 0.5(c_{35}c_{45} - c_{34}c_{55})/\Delta_3 \\ c_3 &= 0.5(c_{44}c_{55} - c_{45}c_{45})/\Delta_3 \end{aligned} \tag{B3}$$

where

$$\begin{aligned} \Delta_1 &= c_{11}c_{55}c_{66} + 2c_{16}c_{15}c_{56} - c_{55}c_{16}^2 - c_{11}c_{56}^2 - c_{66}c_{15}^2 \\ \Delta_2 &= c_{22}c_{44}c_{66} + 2c_{26}c_{24}c_{46} - c_{44}c_{26}^2 - c_{22}c_{46}^2 - c_{66}c_{24}^2 \\ \Delta_3 &= c_{33}c_{44}c_{55} + 2c_{34}c_{45}c_{35} - c_{44}c_{35}^2 - c_{55}c_{34}^2 - c_{33}c_{45}^2 \end{aligned} \tag{B4}$$

Similarly, in the particular solution of stress caused by the body force of gravity, ie., Eqn. (13), the coefficients are

$$
\begin{aligned}
d_{11} &= 1 \\
d_{21} &= 2(a_1c_{12} + a_3c_{25} + a_2c_{26}) \\
d_{31} &= 2(a_1c_{13} + a_3c_{35} + a_2c_{36}) \\
d_{41} &= 2(a_1c_{14} + a_3c_{45} + a_2c_{46}) \\
d_{51} &= 0 \\
d_{61} &= 0
\end{aligned}
\tag{B5}
$$

$$
\begin{aligned}
d_{12} &= 2(b_2c_{12} + b_3c_{14} + b_1c_{16}) \\
d_{22} &= 1 \\
d_{32} &= 2(b_2c_{23} + b_3c_{34} + b_1c_{36}) \\
d_{42} &= 0 \\
d_{52} &= 2(b_2c_{25} + b_3c_{45} + b_1c_{56}) \\
d_{62} &= 0
\end{aligned}
\tag{B6}
$$

$$
\begin{aligned}
d_{13} &= 2(c_1c_{15} + c_2c_{14} + c_3c_{13}) \\
d_{23} &= 2(c_1c_{25} + c_2c_{24} + c_3c_{23}) \\
d_{33} &= 1 \\
d_{43} &= 0 \\
d_{53} &= 0 \\
d_{63} &= 2(c_1c_{56} + c_2c_{46} + c_3c_{36})
\end{aligned}
\tag{B7}
$$

C

1. The exact closed-form solution for a block of height h under uniform and constant compression ($T(t) = T \cdot H(t)$):

For the stresses, the only non-zero component is (Lekhnitskii, 1963):

$$\sigma_{zz} = -T \cdot H(t) \tag{C1}$$

The vertical displacement in the isotropic elasticity can be written as (Lekhnitskii, 1963):

$$u_z = -\frac{T(s)}{E(s)}\left(z - \frac{h}{2}\right) \tag{C2}$$

Where $T(s)$ and $E(s)$ are the Laplace transformed boundary traction and Young's modulus, respectively. For the time-Heaviside compression, the solution in the Laplace transformed domain becomes

$$u_z(s) = -\frac{T}{sE(s)}\left(z - \frac{h}{2}\right) \tag{C3}$$

Inverse of this equation results in the following displacement in the time domain

$$u_z(t) = -\frac{T\{(\lambda + \mu) + (\mu K/v)t\}}{3K\mu}\left(z - \frac{h}{2}\right) \tag{C4}$$

2. The St. Venant's solution for a block of height h resting on a rigid base and under constant gravity ($\rho g \cdot H(t)$) in the z-direction:

For the pure elastic and isotropic case, the vertical displacement can be expressed as (Lekhnitskii, 1963):

$$u_z = -\frac{\rho g}{2E}\left[h^2 - (h - z)^2\right] \tag{C5}$$

In a similar way to the uniform compression case, the following displacement in the time domain can be derived

$$u_z(t) = -\frac{\rho g\{(\lambda + \mu) + (\mu K/v)t\}}{6K\mu}\left[h^2 - (h - z)^2\right] \tag{C6}$$

The vertical stress component in the time domain is

$$\sigma_{zz} = -\rho g(h - z)H(t) \tag{C7}$$

References

Amadei, B.; Pan, E. (1992): Gravitational stresses in anisotropic rock masses with inclined strata. Int. J. Rock Mech. Min. Sci. & Geomech. Abstr., 29: 225–236

Carini, A.; Donato, O. De (1992): Fundamental solutions for linear viscoelastic continua. Int. J. Solids Structures, 29: 2989–3009

Carini, A.; Gioda, G. (1986): A boundary integral equation technique for visco-elastic stress analysis. Int. J. Num. Anal. Meth. Geomech., 10: 585–608

Carini, A.; Diligenti, M.; Maier, G. (1991): Boundary integral equation analysis in linear viscoelasticity: variational and saddle point formulations. Comput. Mech., 8: 87–98

Chave, A. D. (1983): Numerical integration of related Hankel transforms by quadrature and continued fraction expansion. Geophys., 48: 1671–1686

Christensen, U. R. (1987): Some geodynamical effects of anisotropic viscosity. Geophy. J. R. Astr. Soc., 91: 711–736

Cristescu, N. D. (1993): Rock rheology. In "Comprehensive Rock Engineering". Pergamon Press. J. A. Hudson ed., Vol I: 523–544

Davies, B.; Martin, B. (1979): Numerical inversion of the Laplace transform: a survey and comparison of methods. J. Comput. Phys., 33: 1–32

Frassine, R.; Pavan, A. (1990): An application of viscoelastic fracture criteria to steady crack propagation in a polymeric material under fixed deformation. Int. J. Fract., 43: 303–317

Gaul, L.; Schanz, M. (1994): A viscoelastic boundary element formulation in time domain. Arch. Mech., 46: 485–496

Han, D. (1993): A New Analysis of Post Glacial Rebound and an Analysis of Anisotropy of the Mantle Rheology. Ph.D. Thesis, University of Colorado at Boulder

Hanggi, P.; Roesel, F.; Trautmann, P. (1980): Evaluation of infinite series by use of continued fraction expansions: a numerical study. J. Comp. Phys., 37: 252–258

Huang, N. C.; Zhang, L. H.; Nomura, S. A.; Houghton, J. E. (1991): Experiments on crack propagation in a viscoelastic material. Int. J. Fract., 48: 299–309

Kusama, T.; Mitsui, Y. (1982): Boundary element method applied to linear viscoelastic analysis. Appl. Math. Model., 6: 285–290

Lee, E. H. (1955): Stress analysis in viscoelastic bodies. Quart. Appl. Math., 13: 183–190

Lee, S. S. (1995): Boundary element analysis of viscoelastic solids under transient thermal state. Eng. Analy. Bound. Elements, 16: 35–39

Lee, S. S.; Kim, Y. J. (1995): Time-domain boundary element analysis of cracked linear viscoelastic solids. Eng. Fract. Mech., 51: 585–590

Lee, S. S.; Westmann, R. A. (1995): Application of high-order quadrature rules to time-domain boundary element analysis of viscoelasticity. Int. J. Numer. Meth. Eng., 38: 607–629

Lee, S. S.; Sohn, Y. S.; Park, S. H. (1994): On fundamental solutions in time-domain boundary element analysis of linear viscoelasticity. Eng. Analy. Bound. Elements, 13: 211–217

Lekhnitskii, S. G. (1963): Theory of Elasticity of an Anisotropic Elastic Body. Holden-Day, San Francisco

Narayanan, G. V.; Beskos, D. E. (1982): Numerical operational methods for time-dependent linear problems. Int. J. Numer. Meth. Eng., 18: 1829–1854

Pan, E.; Amadei, B. (1996): A 3-D boundary element formulation of anisotropic elasticity with gravity. Appl. Math. Modelling, 20: 114–120

Piessens, R. (1972): A new numerical method for the inversion of the Laplace transform. J. Inst. Math. Appl., 10: 185–192

Schapery, R. A. (1965): A method of viscoelastic stress analysis using elastic solutions. J. Franklin Institute, 279: 268–289

Schulson, E. M.; Hoxie, S. G.; Nixon, W. A. (1989): The tensile strength of cracked ice. Phil. Mag. A, 59: 303–311

Talbot, A. (1979): The accurate numerical inversion of Laplace transforms. J. Inst. Math. Appl., 23: 97–120

Wang, Y.; Crouch, S. L. (1982): Boundary element methods for viscoelastic media. pp. 704–711. In "Proc. US 23rd Sym. Rock Mech.", Berkeley

Warby, M. K.; Walton, J. R.; Whiteman, J. R. (1992): A finite element model of crack growth in a finite body in the context of mode I linear viscoelastic fracture. Computer Meth. Appl. Mech. Eng., 97: 375–397